



OPEN

Effects of green light-emitting diode irradiation on hepatic differentiation of hepatocyte-like cells generated from human adipose-derived mesenchymal cells

Yuhei Waki, Yu Saito , Shuhai Chen, Tetsuya Ikemoto, Takayuki Noma, Hiroki Teraoku, Shinichiro Yamada, Yuji Morine & Mitsuo Shimada


Light-emitting diode (LED) irradiation has been used in the differentiation of mesenchymal stem cells into a variety of cell types. This study investigated the effect of green LED (GLED) irradiation on the differentiation of adipocyte-derived mesenchymal cells into hepatocyte-like cells (HLCs) and the mechanism of its action. HLCs in the hepatocyte maturation phase were irradiated with GLED (520 nm, 21 W/m², 5 min/day for 10 days). The cells were then assessed for expression of hepatocyte maturity genes and opsin 3 (OPN3), hepatocyte function, viability, apoptosis, and levels of reactive oxygen species (ROS), intracellular adenosine triphosphate (ATP) and calcium ions (Ca²⁺). GLED irradiation increased Alpha-1 antitrypsin and Ornithine transcarbamylase gene expression, promoted Cytochrome P450 3A4 activity and urea synthesis, and elevated intracellular ROS, ATP and Ca²⁺ levels. OPN3 expression was significantly more upregulated in GLED-irradiated HLCs than in the non-irradiated HLCs. No significant difference in cell viability or apoptosis was observed between GLED-irradiated and non-irradiated HLCs. GLED irradiation can promote hepatocyte maturation and functions through OPN3. GLED irradiation also stimulated mitochondrial function via Ca²⁺/ATP/ROS activation. GLED irradiation has potential to support cell-based transplantation in patients.

Hepatocyte transplantation has been used as a bridging therapy for patients with metabolic diseases and acute liver failure, mainly in Europe and the United States. However, there are various problems with hepatocyte transplantation, including a shortage of donors, poor cell survival rates following isolation and cryopreservation, and poor long-term cell survival rates after transplantation. To address these donor source problems, the differentiation of hepatocytes from induced pluripotent stem cells, embryonic stem cells, and mesenchymal stem cells (MSCs) has been actively pursued.

We have previously reported methods for inducing differentiation of human adipose tissue-derived mesenchymal stem cells (ADSCs) into hepatocyte-like cells (HLCs), which acquire hepatocyte functions, such as ammonia clearance and CYP3A4 enzyme activity¹. However, our HLCs have inferior hepatocyte function compared with primary hepatocytes, indicating that improved hepatocyte function is necessary for these cells to be used clinically.

Recently, light-emitting diode (LED) irradiation has been used to treat several clinical conditions, including wound healing, pain, bone regeneration and treatment of various diseases and infections². We have reported that LED irradiation can result in various biological effects, such as mouse hepatocyte proliferation and colon cancer cell apoptosis^{3,4}. The effect of LED irradiation at different wavelengths and energy densities also improves the regenerative capacity of various types of MSC^{5,6}. Green LED (GLED) irradiation promotes the differentiation of MSCs into neurons and osteoblasts^{2,7}. However, it is not known whether GLED can promote the hepatic differentiation of HLCs. Therefore, we focused on the effect of GLED on the differentiation of HLCs from ADSCs.

Opsins are G protein-coupled receptors (GPCRs) present in most animals that absorb light to activate visual and non-visual functions⁸. Among seven opsin subtypes, opsin 3 (OPN3) is expressed in various human tissues, including the liver, brain and kidney, in addition to the eye^{9,10}. OPN3 can induce activation of

Department of Surgery, Tokushima University, 3-18-15 Kuramoto-cho, Tokushima 770-8503, Japan. email: saito.yu.1001@tokushima-u.ac.jp

calmodulin-dependent protein kinase (CaMK) and p38 through a GPCR-related phosphorylation pathway¹¹. In addition, CaMK can activate peroxisome proliferator-activated receptor gamma coactivator 1-alpha (PGC-1A), which is a master gene related to mitochondrial metabolism, to cause increased expression of genes involved in urea synthesis, including ornithine transcarbamylase (OTC)¹². However, the effects and mechanisms of GLED irradiation on hepatic differentiation of HLCs generated from ADSCs is unclear. In the present study, therefore, the effects of GLED irradiation on the differentiation of HLCs from ADSCs was investigated, and its mechanism was also explored.

Results

Morphology and cell viability

There were no significant differences in morphology between GLED-irradiated and non-irradiated cells, with both showing morphology similar to our HLCs previously reported¹ (Fig. 1a). As shown in Fig. 1b, live/dead images demonstrated no significant difference between GLED-irradiated and non-irradiated HLCs. Annexin/PI flow cytometry and caspase 3 and 7 gene expression were also not significantly different between the two groups (Fig. 1c and d).

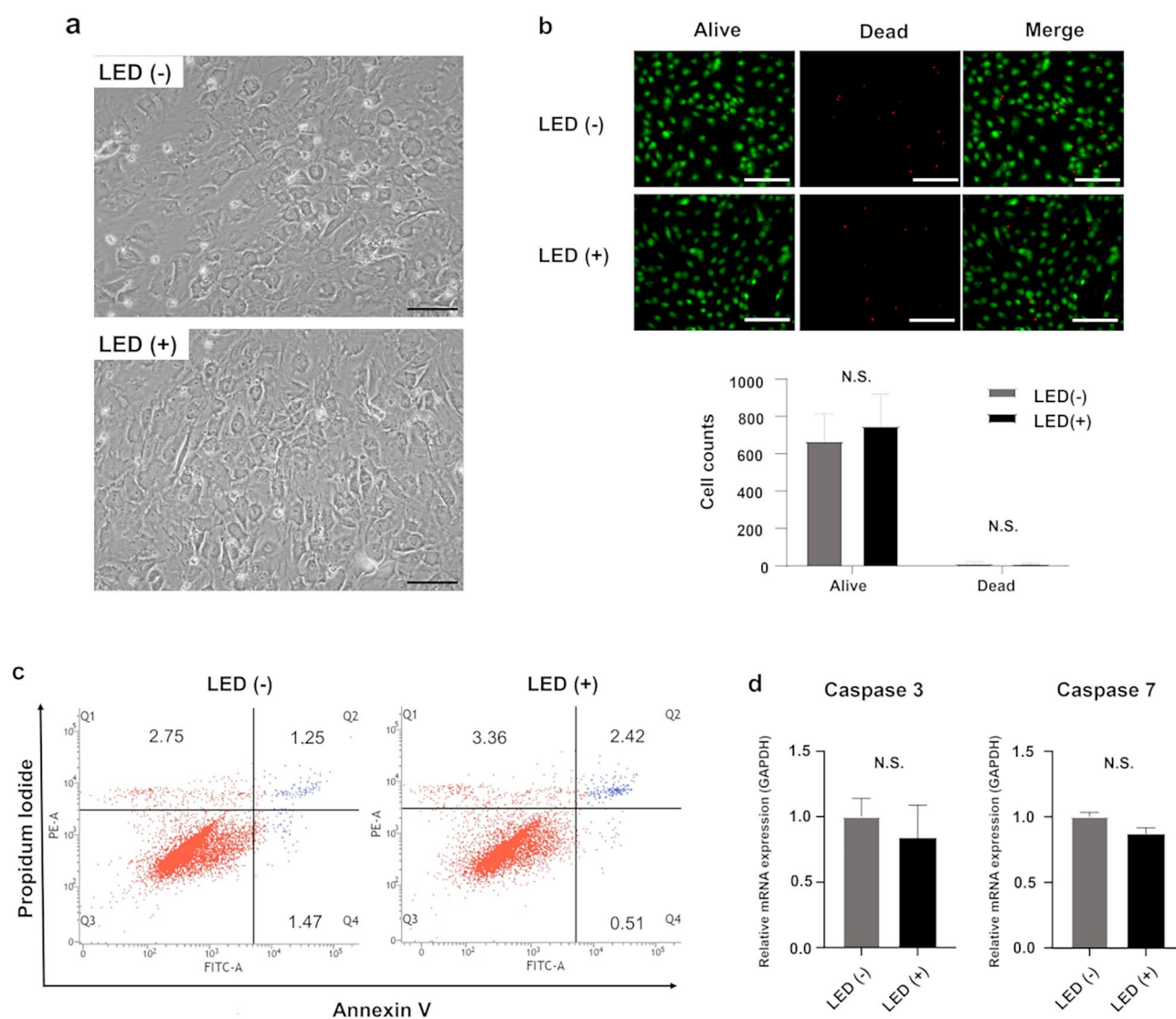


Figure 1. Morphology, viability and apoptosis of HLCs with or without GLED irradiation on day 21. **(a)** The morphology of non-irradiated (LED-) and GLED-irradiated (LED+) HLCs. Scale bar = 100 μm. **(b)** Viability of HLCs irradiated by GLED was assessed by live/dead staining, and no significant difference in viable cell counts between GLED-irradiated and non-irradiated HLCs was observed. Scale bar = 200 μm. **(c)** Annexin/propidium iodide flow cytometry demonstrated no significant difference between GLED-irradiated and non-irradiated HLCs. **(d)** Expression of caspase 3 and 7 genes was not significantly different between GLED-irradiated and non-irradiated HLCs (n = 4). The data are shown as means ± standard deviation. N.S., not significant.

Hepatocyte genes and functions

The levels of *AAT* and *OTC* mRNAs were significantly higher in GLED-irradiated HLCs compared with non-irradiated HLCs but there were no differences in the mRNA levels of *ALB* and *CPS1* between the two groups (Fig. 2a). All the levels of hepatocyte genes of GLED-irradiated HLCs were significantly lower compared to primary human hepatocytes (PHHs) (Fig. 2a). Consistently, GLED irradiation improved both ammonium clearance and CYP3A4 activity in HLCs, but did not reach to PHHs (Fig. 2b). There was no difference between the GLED-irradiated and non-irradiated HLCs in the concentration of albumin in the culture medium on Day 21 (Supplemental Fig. 1).

OPN3 expression

OPN3 expression was evaluated by RT-PCR (Fig. 3a), western blot analysis (Fig. 3b and Supplementary Fig. 2) and immunofluorescence staining (Fig. 3c). Each analysis showed OPN3 to be upregulated in GLED-irradiated HLCs compared with levels in non-irradiated HLCs. Meanwhile, the level of OPN3 expression in GLED-irradiated HLCs was significantly lower compared to PHHs.

Mitochondrial function

Compared with non-irradiated cells, the mRNA level of *PCG1A*, which is a master gene of mitochondrial metabolism, was significantly increased (Fig. 4a) and intracellular ATP production and calcium ions (Ca^{2+}) concentration were higher in GLED-irradiated HLCs (Fig. 4b and c). DCFDA staining was more intense in GLED-irradiated HLCs and flow cytometry assessment showed higher ROS activity in GLED-irradiated HLCs compared with non-irradiated cells (Fig. 4d and e).

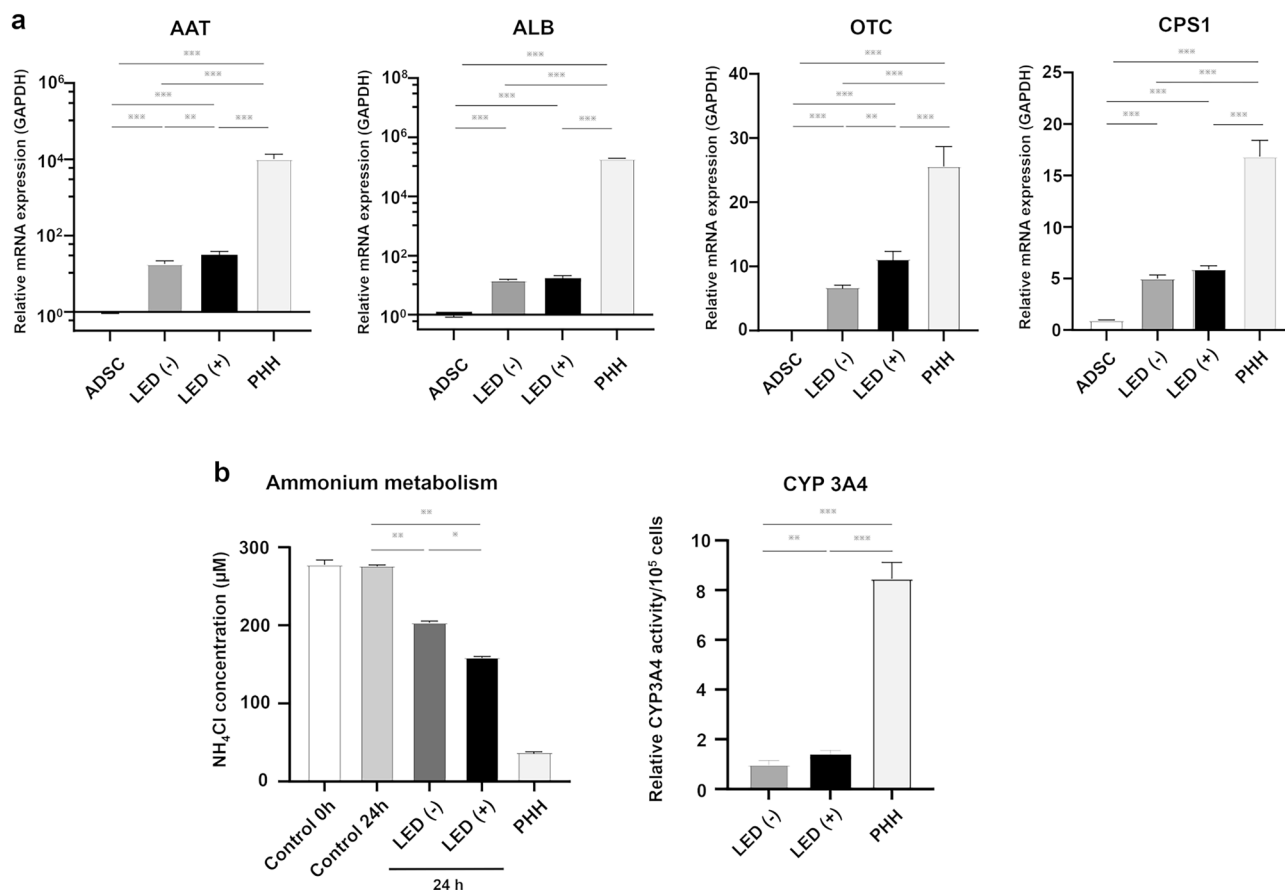


Figure 2. Hepatocyte maturation genes and hepatocyte function in GLED-irradiated and non-irradiated HLCs at day 21. **(a)** RT-PCR showed that *AAT* and *OTC* expression was significantly higher in GLED-irradiated HLCs compared with non-irradiated HLCs ($n=4$). PHHs were used as a positive control ($n=4$). **(b)** Ammonia assays showed significantly higher resolution in GLED-irradiated HLCs than in non-irradiated HLCs, and CYP3A4 activity was significantly higher in GLED-irradiated HLCs than in non-irradiated HLCs, but these hepatocyte functions did not reach to PHHs. The data are shown as means \pm standard deviation. * $P < 0.05$, ** $P < 0.01$ and *** $P < 0.001$. ADSC, adipose tissue-derived mesenchymal stem cell; AAT, alpha-1 antitrypsin transcarbamylase; ALB, albumin; OTC, ornithine transcarbamylase; CPS1, carbamyl phosphate synthase 1, PHH, primary human hepatocyte.

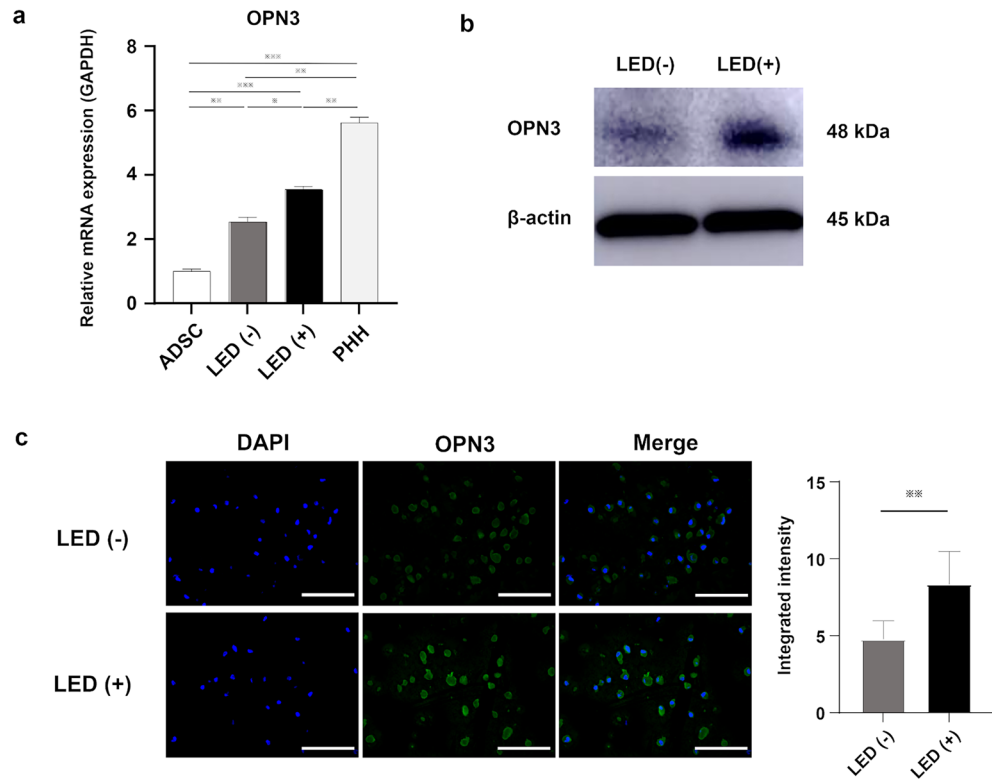


Figure 3. Expression of OPN3 in GLED-irradiated HLCs. **(a)** Gene expression of *OPN3* was significantly higher in GLED-irradiated HLCs than in non-irradiated HLCs ($n=4$). **(b)** Western blotting demonstrated that OPN3 protein expression was more abundant in GLED-irradiated HLCs than in non-irradiated HLCs. **(c)** Fluorescence immunostaining showed higher OPN3 intensity in GLED-irradiated HLCs than in non-irradiated HLCs. The data are shown as means \pm standard deviation. * $P < 0.05$ and ** $P < 0.01$. OPN3, opsin 3, ADSC, adipose-derived stem cell, PHH, primary human hepatocyte.

Discussion

The present study revealed that GLED irradiation of HLCs elevated the expression of hepatocyte maturation and urea synthesis genes, and improved hepatocyte functions, such as ammonia clearance and CYP3A4 activity. Moreover, OPN3 was upregulated by GLED irradiation. As a result, PGC1A gene expression and intracellular ATP, Ca^{2+} and ROS levels were all higher in GLED-irradiated HLCs than in non-irradiated HLCs. Therefore, GLED irradiation may improve hepatocyte maturation and function through OPN3 and Ca^{2+} /ROS/ATP interactions via PGC1A upregulation during the hepatocyte differentiation process.

HLCs derived from ADSCs are considered to have promise as a bridging therapy for metabolic disorder syndrome or acute liver failure following liver transplantation. ADSCs are considered to be an ideal cell source for hepatocytes because their use has no prohibitive ethical issues, they lack genetic damage and can be isolated from a patient with minimal invasiveness. We previously demonstrated that both 2D- and 3D-cultured HLCs can be generated from human ADSCs in 21 days¹. Of these HLCs, 3D-HLCs had comparable hepatocyte function to other reported HLCs, showing similar, but not equivalent, hepatocyte function to primary hepatocytes. Therefore, the differentiation process from ADSCs to HLCs needs improvement¹³.

LED irradiation has positive effects on stimulation of neuronal growth, protection of post-ischemia skeletal muscle, protection of cardiomyocytes, acceleration of wound healing, reduction of the inflammatory response, and stimulation of cell proliferation and differentiation^{3,5,7,14}. Here, we demonstrated that GLED irradiation also has an effect on the function of HLCs. GLED irradiation promoted the expression of hepatocyte maturation genes and hepatocyte functions, such as CYP3A4 activity and ammonia reduction, which might bring HLC function a little closer to those of primary human hepatocytes. A previous study showed that a GLED device working in an incubator enhanced the therapeutic efficacy of human ADSCs by modulating photoreceptor expression to promote advanced wound healing¹⁵. A GLED irradiation device may, therefore, be used in an incubator to improve the hepatocyte function of HLCs.

LEDs are superior to other light resources in their functions of controlling light intensity and wavelength⁴. Previous study has reported that GLED strongly accelerated neural differentiation of human umbilical cord-derived mesenchymal cells, compared to red LED¹⁴. In addition, the optimal energy densities for cell differentiation have reported to range from 0.1 to 6 J/cm²¹⁶. This study demonstrated that GLED irradiation (520 nm, 0.63 J/cm², ten times) promoted hepatic differentiation of HLCs. Meanwhile, the hepatic maturation gene expression of HLCs with GLED irradiation for 10 min (1.26 J/cm²) for ten days was as same as that with non-irradiation

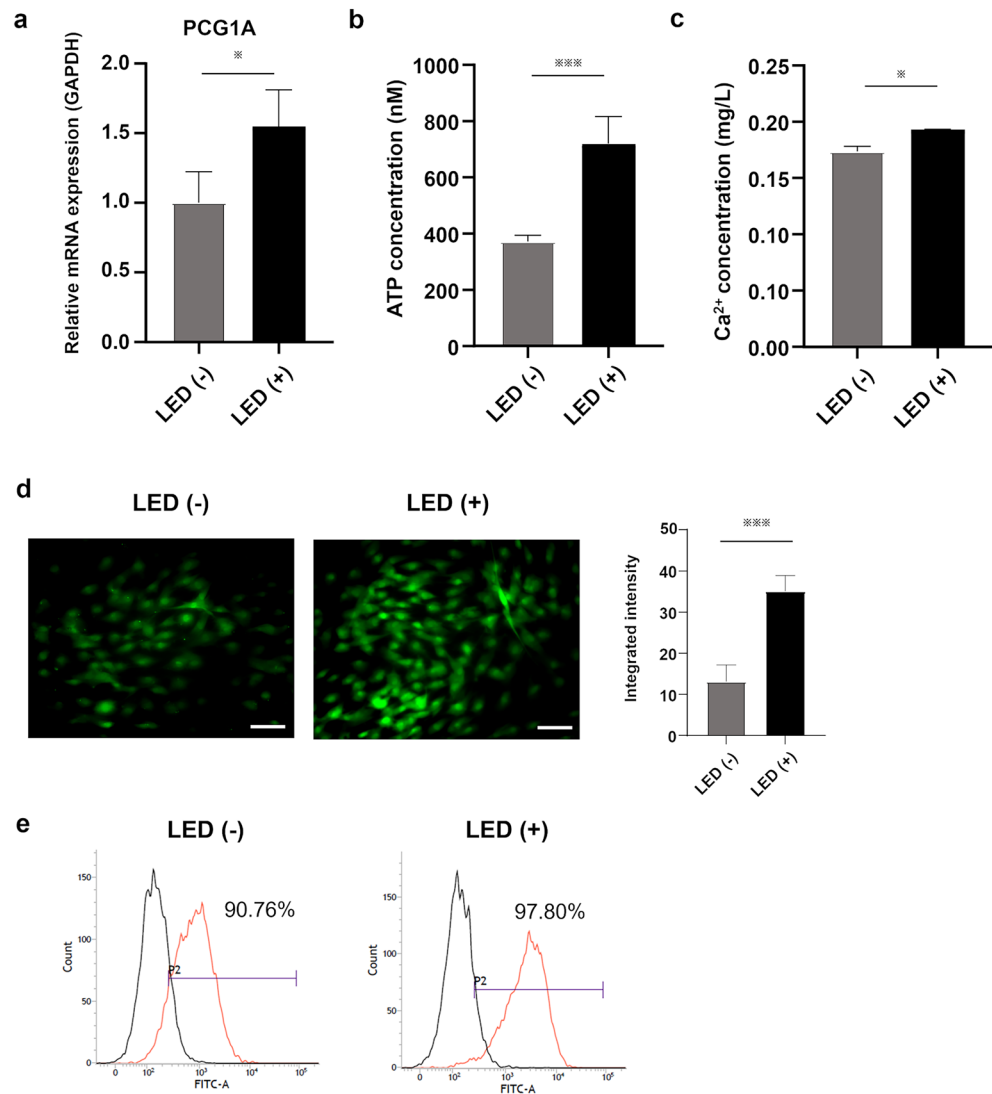


Figure 4. Mitochondrial function in GLED-irradiated HLCs on day 21. **(a)** RT-PCR showed that *PCG1A* expression was significantly higher in GLED-irradiated HLCs compared with non-irradiated HLCs ($n=4$). **(b, c)** GLED-irradiated HLCs exhibited higher levels of intracellular Ca²⁺ and ATP compared with non-irradiated HLCs ($n=4$). **(d)** ROS activity, fluorescently stained with DCFDA, was more intense in GLED-irradiated HLCs than in non-irradiated HLCs. **(e)** Flow cytometry analysis showed a higher percentage of cells with ROS activity for GLED-irradiated HLCs compared with non-irradiated HLCs. The data are shown as means \pm standard deviation. * $P < 0.05$ and *** $P < 0.001$. PGC-1A, peroxisome proliferator-activated receptor gamma coactivator 1- α ; ATP, adenosine triphosphate; ROS, reactive oxygen species; DCFDA, 2',7'-dichlorodihydrofluorescein diacetate.

(Supplemental Fig. 3). Therefore, 5 min' GLED irradiation in the hepatocyte differentiation phase could be effective for hepatic maturation.

GLEDs exert their effects by activating opsins, which are GPCRs associated with several phosphorylation pathways⁸. Increased OPN3 expression by GLED irradiation promotes kinase activation and increased ATP production in human orbital adipose stem cells, and phototransduction through OPN3 regulates the selectivity of phosphorylation by target kinases¹⁷. Additionally, OPN3 can induce CaMK and p38 through a GPCR pathway, and can ultimately upregulate matrix metalloproteinase in human dermal fibroblasts by activating Ca²⁺¹¹. Activation of CaMK and p38 enhances *PCG1A* expression, which promotes the expression of *OTC* and *CPS1*. These genes are involved in urea synthesis and the differentiation of human stem cells into astrocytes^{12,18,19}.

OPN3 significantly increases intracellular ATP or Ca²⁺, which are parameters of mitochondrial function, through activation of transient receptor potential channels, resulting in the generation of ROS^{20,21}. Intracellular Ca²⁺ elevation can cause ROS generation²²; therefore, an increase in intracellular ROS levels may trigger the activation of *OTC* gene transcription in hepatocyte differentiation¹⁶. Importantly, our results of GLED irradiation leading to a significant increase in intracellular ATP and Ca²⁺ levels in HLCs are in line with the above findings.

Therefore, in addition to the OPN3 pathway described above, ROS may be involved in the upregulation of OTC gene expression.

We suggest that GLED irradiation increases CYP3A4 activity by activation of the OPN3 GPCR pathway. These findings provide new insights into the molecular mechanisms underlying the action of hepatic maturation genes. Figure 5 summarizes both the effect of GLED irradiation and its mechanism of action.

There are certain limitations to the present study. The results were based on *in vitro* experiments. Currently, we are planning to transplant our HLCs (non-irradiated) into mouse models of hepatic metabolic disorders. Further investigation is warranted in *in vivo* animal models of hepatic metabolic disorders to evaluate the effects of LED-irradiated HLCs. In conclusion, GLED irradiation can promote hepatocyte maturation and functions through OPN3. GLED irradiation stimulated mitochondrial function via Ca^{2+} /ATP/ROS activation. GLED irradiation might be a potential method to support cell-based transplantation in patients.

Methods

Cell culturing

PHHs were purchased from Thermo Scientific Inc. (Waltham, MA, USA), and cultured using the Hepatocyte Medium (Thermo Scientific Inc.) according to the manufacturer's protocol. PHHs were used for experiments within 3 days after seeding.

HLC generation

STEMPRO human ADSCs were purchased from Life Technologies (Tokyo, Japan). Our HLC generation protocol has been reported¹. ADSCs were used in experiments at passages 2–6. Briefly, ADSCs (2×10^6 per well) were seeded in 6-well flat-bottomed collagen-coated plates (Nunclon Sphera Microplates, Thermo Scientific Inc.) and incubated with serum-free Dulbecco's modified Eagle's medium with F-12 Supplement (DMEM/F-12) for 24 h. Thereafter, our three-step differentiation protocol was performed. In the first step, to induce definitive endoderm differentiation, cells were incubated with DMEM/F-12 containing 0.5 mg/ml bovine serum albumin fraction V (BSA; Sigma-Aldrich, St. Louis, MO, USA) and 2 $\mu\text{mol/L}$ Chir99021 (a glycogen synthase kinase 3 inhibitor; Selleckchem, Tokyo, Japan) for 24 h. The following day, 1% insulin-transferrin-selenium (ITS, Sigma-Aldrich) was added to the medium. In the second step, for hepatoblast differentiation, the medium was changed to minimum essential medium with non-essential amino acids (Thermo Scientific Inc.) containing 0.5 mg/ml BSA, 1% ITS, 20 ng/ml bone morphogenic protein 2 (PeproTech, Inc. NJ, USA), and 30 ng/ml fibroblast growth factor 4 (PeproTech, Inc.) and incubation continued for 5 days. In the third step, for induction of hepatocyte differentiation, the cells were treated with 20 ng/ml hepatocyte growth factor (PeproTech, Inc.) for 5 days, followed by treatment with 20 ng/ml hepatocyte growth factor, 10 ng/ml oncostatin M (PeproTech, Inc.) and 1×10^{-6} M dexamethasone (Sigma-Aldrich) for another 5 days.

GLED irradiation

An LED irradiation device (3LH-256/3LH-75DPS, Nippon Medical & Chemical Instruments Co., Ltd., Osaka Japan) was used to produce GLED with a wavelength of 520 nm at maximum light intensity. A photoradiometer (Light analyzer LA-105, Nippon Medical & Chemical Instruments Co., Ltd.) was used to measure the light

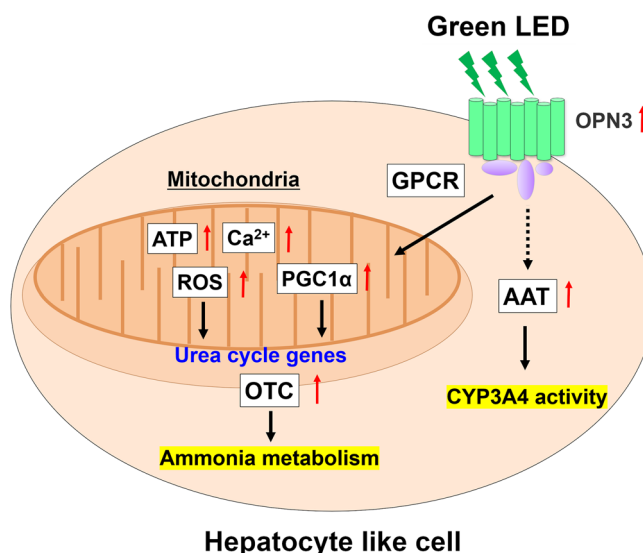


Figure 5. Schematic representation of proposed mechanisms underlying improved hepatocyte maturation and function in response to GLED irradiation of HLCs. OPN3, opsin 3; GPCR, G protein-coupled receptor; AAT, alpha-1 antitrypsin transcarbamylase; OTC, ornithine transcarbamylase; ATP, adenosine triphosphate; ROS, reactive oxygen species; peroxisome proliferator-activated receptor gamma coactivator 1-alpha, PGC-1A.

intensity. The cell culture plates were placed on the LED irradiation device and energy density generation was set at 21 W/m². Cells were exposed to GLED in the third step (hepatocyte differentiation phase) at room temperature for 5 min which gave a radiant exposure of 0.63 J/cm² for each day. The GLED irradiation protocol is shown in Fig. 6. Control group cells were treated in the same manner except for no GLED exposure. Sufficient ventilation was provided to ensure that the temperature of the culture medium did not change during treatment. The experiments were replicated at least 3 times under the same conditions with three purchased ADSCs.

Cell viability

The LIVE/DEAD Cell Imaging Kit (Thermo Fisher Scientific, Inc.) was used to determine the live/dead nucleated cells among GLED-treated and non-treated HLCs at day 21, following the manufacturer's protocol. The fluorescence signals were measured using a fluorescence microscope (Keyence Corporation). Cells were counted using Image J software (ver. 1.53, National Institutes of Health, Bethesda, MD, USA).

Apoptosis detection by flow cytometry

Flow cytometry was used to detect apoptosis. Both irradiated and non-irradiated cells were labeled with Annexin V-conjugated fluorescein isothiocyanate and propidium iodide (PI) using a MEBCYTO Apoptosis Kit according to the manufacturer's instructions (MBL international, Woburn, MA, USA). Quantitative analysis was performed using a FACSVerse cytometer and FACSuite software (Becton Dickinson, Franklin Lakes, NJ, USA).

RT-PCR of HLCs

Total RNA was prepared from each HLC sample using the RNeasy Mini Kit (Qiagen, Hilden, Germany) according to the manufacturer's instructions. cDNA was synthesized using a reverse transcription kit (Applied Biosystems, Foster City, CA, USA). The following TaqMan assays (with assay identification number and primers) were used: alpha-1 antitrypsin (AAT) (Hs00165475_m1), albumin (ALB) (Hs00910225_m1), OTC (Hs00166892_m1), carbamyl phosphate synthase 1 (CPS1) (Hs00157048_m1), OPN3 (Hs00173892_m1) and PGC-1A (Hs00173304_m1). GAPDH (Hs02786624_g1) was used as an internal control with stable level of expression for normalization (Supplemental Table 1). All primers were purchased from Thermo Fisher Scientific, Inc. The data were analyzed using the 2^{-ΔΔCt} method. Relative expression levels were calculated as ratios to GAPDH expression. The results are presented as the fold change of the relative mRNA expression for a group compared with that in the control group.

Western blotting

RIPA buffer (Thermo Fisher Scientific, Inc.) containing a protease inhibitor cocktail (Sigma- Aldrich) and a PhosSTOP phosphatase inhibitor cocktail (Roche, Tokyo, Japan) was used for protein extraction. Total protein concentrations were assessed with a BCA Kit (Thermo Fisher Scientific, Inc.) and equal quantities of extracted proteins were separated on 10% sodium dodecyl sulfate–polyacrylamide gel electrophoresis gels and transferred to polyvinylidene difluoride membranes (Bio-Rad, Hercules, CA, USA). To evaluate protein abundance, blots were blocked with 5% skimmed milk for 1 h at room temperature and incubated overnight at 4 °C with the following primary antibodies: anti-OPN3 (1:1,000; SAB2700986; Sigma-Aldrich) and anti-β-actin (1:1,000; cat. no. 4970; Cell Signaling Technology, Inc. MA, USA). Blots were then incubated with anti-rabbit IgG, HRP-linked (1:2,000; cat. no. 7074; Cell Signaling Technology, Inc.) as the secondary antibody for 1 h at room temperature. The proteins were detected with chemiluminescence (GE, Little Chalfont, Buckinghamshire, UK).

CYP3A4 activity assay

CYP3A4 enzyme activity was assessed using the P450- Glo™ CYP3A4 Assay with Luciferin-IPA (Promega Corporation, WI, USA) according to the manufacturer's instructions. Luminescence was measured using a microplate reader (SpectraMax i3; Molecular Devices, LLC). Luminescent measurements were normalized to the total amount of viable cells.

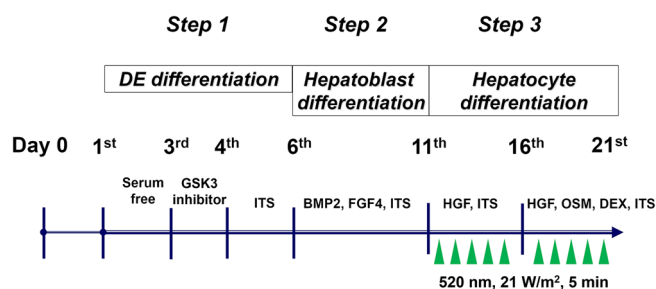


Figure 6. Study protocol of GLED-irradiated HLCs. GLEDs were irradiated once a day for 5 min at 21 W/m² during the 10 days of the hepatocyte differentiation phase. DE, definitive endoderm; GSK, glycogen synthase kinase; ITS, insulin-transferrin-selenium; BMP, bone morphogenic protein; FGF, fibroblast growth factor; HGF, hepatocyte growth factor; OSM, oncostatin M; DEX, dexamethasone.

Ammonium metabolism assay

Ammonium metabolism was evaluated by the change in ammonium ion concentration in the cell culture supernatant at 24 h after the addition of ammonium chloride (NH₄Cl). Briefly, NH₄Cl (FUJIFILM Wako Pure Chemical Corporation) diluted with Hanks' Balanced Salt Solution (HBSS, FUJIFILM Wako Pure Chemical Corporation) to a standard of 300 μmol/L was added to culture plates after the plates were washed twice with HBSS. The plates were placed adjacent to each other in the same incubator and incubated under the same conditions. The supernatants were then collected and applied to an ammonia assay kit (Cell Biolabs) to measure ammonium concentrations at 24-h intervals after NH₄Cl addition. Controls were culture plates containing only standard ammonia solution. As a reference value, ammonium metabolism assays were performed using PHHs with Hepatocyte Medium in the same manners described above.

Immunofluorescence staining

HLCs were immobilized in iPCell (Geno staff, Tokyo, Japan) and fixed with 4% paraformaldehyde according to the manufacturer's protocol. Frozen jellified cells were then sectioned, mounted on glass slides and incubated with an anti-OPN3 primary antibody (Abcam, ab140901) overnight at 4 °C. Cells were then incubated with a fluorophore-conjugated secondary antibody (Thermo Fisher Scientific Inc., A11008) and then with DAPI (Thermo Fisher Scientific Inc., P306931). Slides were observed under a fluorescence microscope (Keyence Corporation, Itasca, IL, USA).

Ca²⁺ and ATP assays

Intracellular Ca²⁺ concentration in GLED-treated HLCs was measured using a Ca²⁺ detection assay kit (Abcam, Cambridge, UK). Briefly, after cell homogenization and centrifugation at 20,000 × g for 5 min at 4 °C, supernatants were collected. Samples were mixed with chromogenic reagent and incubated at room temperature for 10 min according to the manufacturer's protocol. The absorbance values of each sample were then measured at 575 nm with a microplate reader. Measurements for each cell lysate sample were standardized at 1 × 10⁶ HLCs.

To evaluate the amount of ATP in GLED-treated and non-treated HLCs, cell homogenization and centrifugation was performed as for the above Ca²⁺ assay and an adenosine triphosphate (ATP) assay kit (FUJIFILM Wako Pure Chemical Corporation) was used according to the manufacturer's protocol. Measurements for each cell lysate sample were standardized at 1 × 10⁶ HLCs.

Detection of reactive oxygen species (ROS)

The ROS Assay Kit (Dojindo Lab., Kumamoto, Japan) was used to measure the formation of intracellular ROS. Briefly, HLCs on differentiation day 21 (10 days after GLED irradiation) were seeded into a 6-well dish and incubated with 2',7'-dichlorodihydrofluorescein diacetate (DCFDA) for 30 min in the dark at 37 °C. After washing twice with HBSS, the cells were incubated with 100 μmol/L hydrogen peroxide for 30 min according to the manufacturer's protocol. The fluorescence signals were measured and analyzed using a FACSVerse cytometer and FACSuite software (Becton Dickinson). A fluorescence microscope (Keyence Corporation) was used to image cells and the level of cellular fluorescence was measured using the Cell Magic Wand plugin for Image J software.

Statistical analysis

All data are presented as the mean ± standard difference. Statistical analysis and graph production were conducted using GraphPad Prism v7.0 (GraphPad Software, Inc.) and Image J software. Comparisons between two groups were analyzed using the Mann-Whitney test. P-values less than 0.05 (two-sided) were considered statistically significant.

Data availability

The data that support the findings of this study are available from the corresponding author upon reasonable request.

Received: 31 May 2023; Accepted: 26 October 2023

Published online: 15 November 2023

References

- Saito, Y. *et al.* Effective three-dimensional culture of hepatocyte-like cells generated from human adipose-derived mesenchymal stem cells. *J. Hepatob. Pancreat. Sci.* **28**(9), 705–715 (2021).
- Seyyedini, S., Shojaei, M., Fallah, H., Khosravi, A. & Nematollahi-Mahani, S. N. Effects of green light-emitting diode irradiation on neural differentiation of human umbilical cord matrix-derived mesenchymal cells; involvement of MAPK pathway. *Biochem. Biophys. Res. Commun.* **637**, 259–266 (2022).
- Feng, R. *et al.* Photobiomodulation with red light-emitting diodes accelerates hepatocyte proliferation through reactive oxygen species/extracellular signal-regulated kinase pathway. *Hepatol. Res.* **48**(11), 926–936 (2018).
- Matsumoto, N. *et al.* Effect of light irradiation by light emitting diode on colon cancer cells. *Anticancer Res.* **34**(9), 4709–4716 (2014).
- Chang, S. Y., Carpena, N. T., Kang, B. J. & Lee, M. Y. Effects of photobiomodulation on stem cells important for regenerative medicine. *Med. Lasers Eng. Basic Res. Clin. Appl.* **9**, 134–141 (2020).
- Mansano, B. S. D. M. *et al.* Enhancing the therapeutic potential of mesenchymal stem cells with light-emitting diode: Implications and molecular mechanisms. *Oxid. Med. Cell. Longevity* **2021**, 6663539 (2021).
- Higuchi, A. *et al.* Osteoblast differentiation of amniotic fluid-derived stem cells irradiated with visible light. *Tissue Eng. Part A* **17**(21–22), 2593–2602 (2011).
- Sugihara, T., Nagata, T., Mason, B., Koyanagi, M. & Terakita, A. Absorption characteristics of vertebrate non-visual Opsin, Opn3. *PLOS ONE* **11**(8), e0161215 (2016).

9. Blackshaw, S. & Snyder, S. H. Encephalopsin: A novel mammalian extraretinal opsin discretely localized in the brain. *J. Neurosci.* **19**(10), 3681–3690 (1999).
10. Halford, S. *et al.* Characterization of a novel human opsin gene with wide tissue expression and identification of embedded and flanking genes on chromosome 1q43. *Genomics* **72**(2), 203–208 (2001).
11. Lan, Y., Wang, Y. & Lu, H. Opsin 3 is a key regulator of ultraviolet A-induced photoaging in human dermal fibroblast cells. *Br. J. Dermatol.* **182**(5), 1228–1244 (2020).
12. Li, L. *et al.* PGC-1 α promotes ureagenesis in mouse periportal hepatocytes through SIRT3 and SIRT5 in response to glucagon. *Sci. Rep.* **6**, 24156 (2016).
13. Luce, E., Messina, A., Duclos-Vallée, J.-C. & Dubart-Kupperschmitt, A. Advanced techniques and awaited clinical applications for human pluripotent stem cell differentiation into hepatocytes. *Hepatology* **74**(2), 1101–1116 (2021).
14. Dehghani-Soltani, S., Shojaee, M., Jalalkamali, M., Babae, A. & Nematollahi-Mahani, S. N. Effects of light emitting diode irradiation on neural differentiation of human umbilical cord-derived mesenchymal cells. *Sci. Rep.* **7**(1), 9976 (2017).
15. Lee, S. H., Kim, Y. J., Kim, Y. H., Kim, H. Y. & Bhang, S. H. Enhancing therapeutic efficacy of human adipose-derived stem cells by modulating photoreceptor expression for advanced wound healing. *Stem Cell Res. Ther.* **13**(1), 215 (2022).
16. Zamani, A. R. N. *et al.* Modulatory effect of photobiomodulation on stem cell epigenetic memory: A highlight on differentiation capacity. *Lasers Med. Sci.* **35**(2), 299–306 (2020).
17. Ong, W. K. *et al.* The activation of directional stem cell motility by green light-emitting diode irradiation. *Biomaterials* **34**(8), 1911–1920 (2013).
18. Iwata, K., Ferdousi, F., Arai, Y. & Isoda, H. Interactions between major bioactive polyphenols of sugarcane top: Effects on human neural stem cell differentiation and astrocytic maturation. *Int. J. Mol. Sci.* **23**(23), 15120 (2022).
19. Wu, H. *et al.* Regulation of mitochondrial biogenesis in skeletal muscle by CaMK. *Science* **296**(5566), 349–352 (2002).
20. Serrage, H. *et al.* Under the spotlight: Mechanisms of photobiomodulation concentrating on blue and green light. *Photochem. Photobiol. Sci.* **18**(8), 1877–1909 (2019).
21. Wang, Y., Huang, Y.-Y., Wang, Y., Lyu, P. & Hamblin, M. R. Photobiomodulation (blue and green light) encourages osteoblastic differentiation of human adipose-derived stem cells: Role of intracellular calcium and light-gated ion channels. *Sci. Rep.* **6**(1), 33719 (2016).
22. Gordeeva, A. V., Zvyagilskaya, R. A. & Labas, Y. A. Cross-talk between reactive oxygen species and calcium in living cells. *Biochem. (Moscow)* **68**(10), 1077–1080 (2003).

Acknowledgements

The authors would like to thank Mr. Horikawa, Ms. Hara and Ms. Horikawa for technical assistance. We also thank Jeremy Allen, PhD, from Edanz (<https://jp.edanz.com/ac>) for editing a draft of this manuscript.

Author contributions

Y.S. and M.S. conceived the study and supervised the project. Y.W. performed the experiments, analyzed and interpreted the data and wrote the original draft of the manuscript. Y.S., S.C., T.I., T.N., H.T., S.Y., Y.M. and M.S. were also involved in data analysis and final manuscript preparation. All authors reviewed and agreed to the published version of the manuscript.

Competing interests

The authors declare no competing interests.

Additional information

Supplementary Information The online version contains supplementary material available at <https://doi.org/10.1038/s41598-023-45967-7>.

Correspondence and requests for materials should be addressed to Y.S.

Reprints and permissions information is available at www.nature.com/reprints.

Publisher's note Springer Nature remains neutral with regard to jurisdictional claims in published maps and institutional affiliations.



Open Access This article is licensed under a Creative Commons Attribution 4.0 International License, which permits use, sharing, adaptation, distribution and reproduction in any medium or format, as long as you give appropriate credit to the original author(s) and the source, provide a link to the Creative Commons licence, and indicate if changes were made. The images or other third party material in this article are included in the article's Creative Commons licence, unless indicated otherwise in a credit line to the material. If material is not included in the article's Creative Commons licence and your intended use is not permitted by statutory regulation or exceeds the permitted use, you will need to obtain permission directly from the copyright holder. To view a copy of this licence, visit <http://creativecommons.org/licenses/by/4.0/>.

© The Author(s) 2023